17th World Conference on Earthquake Engineering, 17WCEE
Sendai, Japan - September 13th to 18th 2020

DAMAGE TO TELECOMMUNICATION FACILITIES IN THE 2016 KUMAMOTO EARTHQUAKE

M. Okutsu[(1)], A. Ito[(2)] , K. Itasaka[(3)] , M. Tanaka[(4)] , G. Shoji[(5)] , T. Suzuki[(6)]

[(1)] *Senior Research Engineer, Nippon Telegraph and Telephone Corp., masaru.okutsu.ef@hco.ntt.co.jp*
[(2)] *Research Engineer, Nippon Telegraph and Telephone Corp., akira.itou.dp@hco.ntt.co.jp*
[(3)] *Senior Research Engineer, Adviser, Nippon Telegraph and Telephone Corp., kouji.itasaka.nd@hco.ntt.co.jp*
[(4)] *Project Manager, Nippon Telegraph and Telephone Corp., minoru.tanaka.hw@hco.ntt.co.jp*
[(5)] *Profeesor, University of Tsukuba, gshoji@kz.tsukuba.ac.jp*
[(6)] *Professor, Toyo University, tsuzuki@toyo.jp*

…

Abstract

In April 2016, a series of earthquakes occurred in Kumamoto Prefecture, Japan, including two large earthquakes with a Japan Meteorological Agency (JMA) seismic intensity of 7. In the area along the fault, large tremors occurred, many buildings were damaged, and much social infrastructure was damaged. The damage to telecommunication services affected approximately 2,100 lines and nine relay cable sections.

After the Kumamoto Earthquake, telecommunication conduits covering more than 700 km were checked with test pieces, and in-pipe inspection cameras were used for detailed inspection. In this paper, we focus on the damage situation and analysis of such conduits. The damage forms of conduits are classified into joint crushing, joint pull-out, breakage, sediment inflow, bending, and flattening. The conduit damage rate, defined as [number of affected spans] / [number of inspected spans], was 0.06 for the Kumamoto Earthquake. Communication pipes vary in their materials, joints, coatings, and so on, and multiple combinations are mixed and laid in the same plane. Therefore, we analyzed the relationships between damage and various attributes of communication conduits, seismic motion indicators, and micro-topography classification. The seismic motion index was estimated in 250-m grid units from the observed strong motion data, micro-topography classification, surface-layer amplification, and other factors.

The conduit damage rate was almost flat in the range where the seismic motion index (i.e., the seismic intensity scale, measured seismic intensity, PGV, PGA, and SI) was small, but it tended to increase rapidly when it exceeded a certain level. In addition, damage analyses of conduits were conducted in Mashiki, where the earthquake motion was large and many surface earthquake faults appeared. As a result, the damage rate was very high for conduits intersecting surface earthquake faults, but it decreased with increasing distance from such faults. The damage rate for each pipe type is defined as [number of damaged pipes] / [number of inspected pipes]. The damage rate for steel pipe and PVC (i.e., hard vinyl) pipe with large amounts of equipment and old standards was approximately 0.04. In comparison, the damage rate for current standard pipe with expansion/contraction capability was about 0.03. In addition, the damage rate tended to increase as the length of the earthquake increased, as seen for major earthquakes in the past.

The contribution of each attribute to the damage rate was calculated from the quantitative relationship between each attribute and the damage rate. NTT has developed and introduced a conduit-damage prediction method for grasping the priority of earthquake resistance measures for existing conduits and enabling early detection of damaged areas immediately after a major earthquake. We are working to improve the accuracy of the method, reflecting the knowledge obtained in this study.

Keywords: The Kumamoto Earthquake, telecommunication, conduit, damage analysis

1. Introduction

The 2016 Kumamoto Earthquake, with major tremors occurring on April 14 and 16, 2016, caused much damage to communications facilities, as listed in Table **1**[1]. It is important for lifeline operators to analyze the damage caused by earthquakes, derive conditions that are likely to cause earthquake damage, and take corresponding measures against earthquakes that are expected to occur in the future. Yamazaki et al. [2] investigated and analyzed the damage to telecommunications facilities during the 2011 Great East Japan Earthquake. They found that damage began to occur at a Japanese seismic intensity of 5 or more, and that the damage rate tended to increase sharply at a seismic intensity of 6 or more. Shoji et al. [3] analyzed underground communication conduits damaged by the Great East Japan Earthquake, Zhang et al. [4] analyzed underground communication conduits damaged by several inland earthquakes, respectively by focusing on pipe types, conduit lengths, micro-topographic classification, and ground motion, and they clarified the following points: The relationship between the peak ground velocity (PGV) and damage rate is strong. The damage rate for the plug-in joint type is lower than for other joint types. Finally, alluvial lowlands, landfill, and reclaimed land are highly subject to damage.

Following the above, this paper analyzes and considers the damage to underground telecommunication conduits in the 2016 Kumamoto Earthquake, along with the attributes of pipes, ground-motion intensity, micro-topographic classification, and spatial relationships with surface earthquake faults.

Table 1 Outline of damage to telecommunication facilities in the Kumamoto Earthquake

	Number of failures	Cable		Utility pole	Buildings with power outages
		Relay	Subscription		
Damage	4,708	9 sections	Approx. 630	Approx. 1400	45

2. Data used for analysis

The communication conduits for analysis are facilities for accommodating and protecting underground communication cables. They are mainly buried about 1 m below roads and sidewalks. They connect between maintenance holes, which are used for cable connection and branching. The total length of such conduits is approximately 620,000 km nationwide.

Given reports of abnormalities such as cracks, steps, and liquefaction near the locations of underground equipment, as confirmed by emergency visual inspection, and given seismic intensity information for each municipality, as announced by the Japan Meteorological Agency (JMA), direct inspection of underground facilities was performed according to the inspection policy listed in Table 2.

Table 2 Inspection policy for underground telecommunication facilities after the Kumamoto Earthquake

JMA seismic intensity		7	6+	6-	5+≧
Emergency visual inspection result	Abnormal	All			
	Normal		Filtering		

For underground conduits, a test was first conducted with a test piece to understand the damage situation. In a case of failure, an inspection was then conducted with a pipe camera. These inspections extended over 700 km. In this study, detachment, breakage, bending, flattening, and sediment inflow were assumed to be earthquake damage, according to the inspection results with the pipe camera, while failure due to corrosion was excluded. In communication conduits, multiple pipes are usually laid in multiple rows between manholes. Within one span, if even one pipe was damaged, the whole conduit was considered damaged. The damage rate R is expressed as the number of spans with damage divided by the number of spans inspected.

2.1 Attributes of communication conduits

The materials of communication pipes are roughly classified into cast iron, carbon steel, and polyvinyl chloride (PVC, or simply "vinyl"). The ratios of the cumulative construction volume are approximately 0.5 for steel, 0.4 for vinyl, and 0.1 for cast-iron and other types. There have been several changes to joint structures and coatings, and pipes of various specifications have been mixed. Communication conduits were constructed in large quantities from the 1960s to the 1980s, so a large number of facilities were constructed more than 30 years ago. Note that communication conduits are intended to protect and house cables and thus do not require air tightness, unlike a fluid transport pipe. Therefore, many old conduits have low seismic resistance. Table 3 summarizes the pipes' characteristics. The span length of a communication conduit indicates the distance along the pipe axis between the centers of two manholes. This distance is used for matching the design of the cable length and is not a strict pipe length.

Table 3 Pipes used for telecommunication conduit

	Cast-iron pipe	Steel pipe	Hard vinyl pipe
Material	Cast iron Ductile cast iron	Carbon steel	Polyvinyl chloride
Outer diameter (mm)	91.0～96.6	89.1	96.0
Wall thickness (mm)	5.2～8.0	4.2	6.5
Length (m)	3.0, 4.0	4.5, 5.5	5.5
Pipe type * Abbreviations in parentheses	Spigot-joint / screw-joint cast-iron pipe (I) Push-on lock cast-iron pipe (PL-I)	Threaded-joint jute-wound steel pipe (SA) Threaded-joint polyethylene-coated steel pipe (PS) Push-on lock-joint polyethylene-coated steel pipe (PL-PS)	Adhesive-joint hard vinyl pipe (V) Push-on lock hard vinyl pipe (PV)

2.2 Seismic-motion spatial distribution data

Following the method of Suetomi et al. [5], index values of the ground motion intensity, peak ground acceleration (PGA), and PGV were calculated using strong-motion observation data obtained from the K-NET and KiK-net [6] seismic networks of the National Research Institute for Earth Science and Disaster Resilience (NIED) and Japan Meteorological Agency (JMA) [7] stations. First, the amplification degree of the surface layer was calculated using a topographic classification with a 250-m mesh and the average shear-wave velocity to a depth of 30 m (AVS30). This information is published as basic data in J-SHIS [8], by NIED. Next, the maximum acceleration and maximum velocity of the engineering base surface at each observation point were calculated from the observed values and the amplification. Using the ground-motion data obtained through this process, we estimated the ground motion with a 250-m mesh by applying the Kriging method, which interpolates the error from observed values, with the distance attenuation equation of Kataoka et al. [9] For the PGA, the acceleration waveform on the three axes of EW, NS, and UD was synthesized, and the maximum acceleration was adopted. For the PGV, the velocity waveforms in the two horizontal directions, EW and NS, were synthesized, and the maximum velocity was adopted. The index values of the ground motion acting on an underground pipe were set to the PGA and PGV in the 250-m mesh at the center of each span.

Liquefaction was determined using a liquefaction occurrence point survey conducted by NIED [10]. For the surface earthquake faults, data from the National Institute of Advanced Industrial Science and Technology (AIST) [11, 12] was used.

3. Relationships between various attributes and conduit damage

Table 4 summarizes the damage situation of the communication conduits in the Kumamoto Earthquake. Of the 4747 surveyed spans, 271 were affected. There were 147 and 4586 spans with and without liquefaction, respectively. The damage rate was 0.06 total, with rates of 0.12 with liquefaction and 0.06 without liquefaction. The damage rate with liquefaction was higher than that without liquefaction.

Fig. 1 shows the distribution of the communication conduits. The red lines represent damaged spans, the green lines represent undamaged spans, the blue lines represent surface earthquake faults, and the pink rectangle represents the 250-m mesh values for liquefaction. Fig. 2 shows some examples of conduit damages.

Table 4 Overviews of telecommunication conduit damage in the Kumamoto Earthquake

	No damage	Damage	Total	Damage rate
With liquefaction	129	18	147	0.12
Without liquefaction	4333	253	4586	0.06
Total	4462	271	4733	0.06

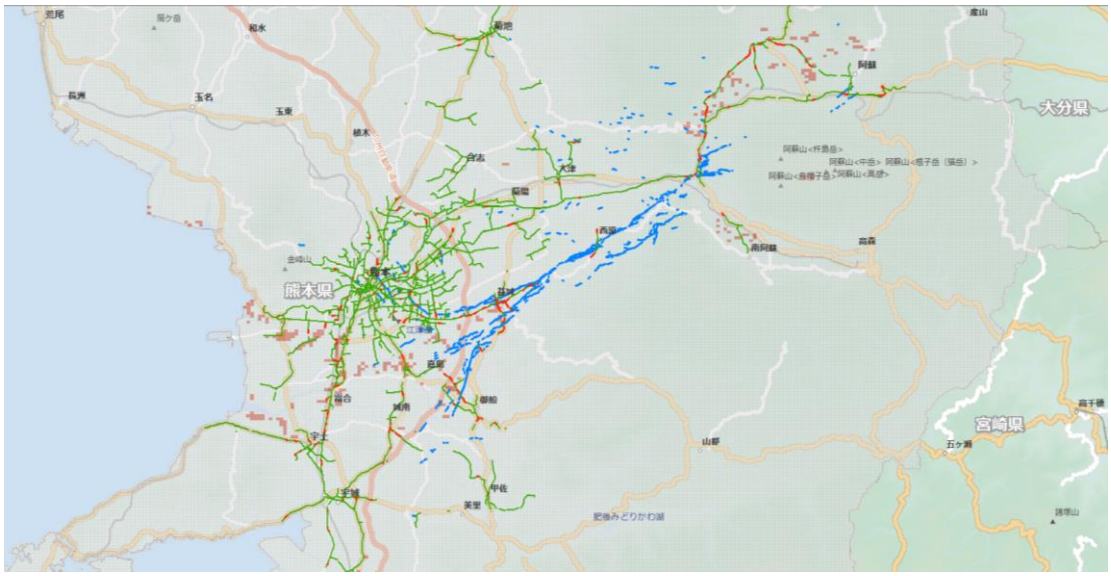

Fig. 1 Distribution of inspected conduits

(a) Threaded-joint (b) Adhesive-joint (c) Large deformation

Fig. 2 Examples of conduit damage

3.1. Seismic motion

First, the characteristics of the ground-motion intensity and the damage to communication conduits were analyzed. Fig. 3 shows relationship between conduit damage and seismic motion index. In the following figures, instances of damage are classified as "with liquefaction" and "without liquefaction." Because there were many data instance without liquefaction, the overall tendency was similar to that case.

The damage rate was almost the same until the intensity of the seismic motion reached a certain value, and then it tended to increase from that value. In cases with liquefaction, the damage rate was higher in areas where the PGA was more than 800 cm/s^2 and areas where the PGV was more than 150 cm/s. We must carefully consider this result, however, because the number of data instances was small. In cases without liquefaction, the damage rate tended to increase when the PGA exceeded 900 cm/s^2 and the PGV exceeded 120 cm/s. As for the JMA seismic intensity, damage started to appear from just over 5+, remained almost the same up to 6+, and rapidly increased at 7. This tendency is similar to the findings of Yamazaki et al[2].

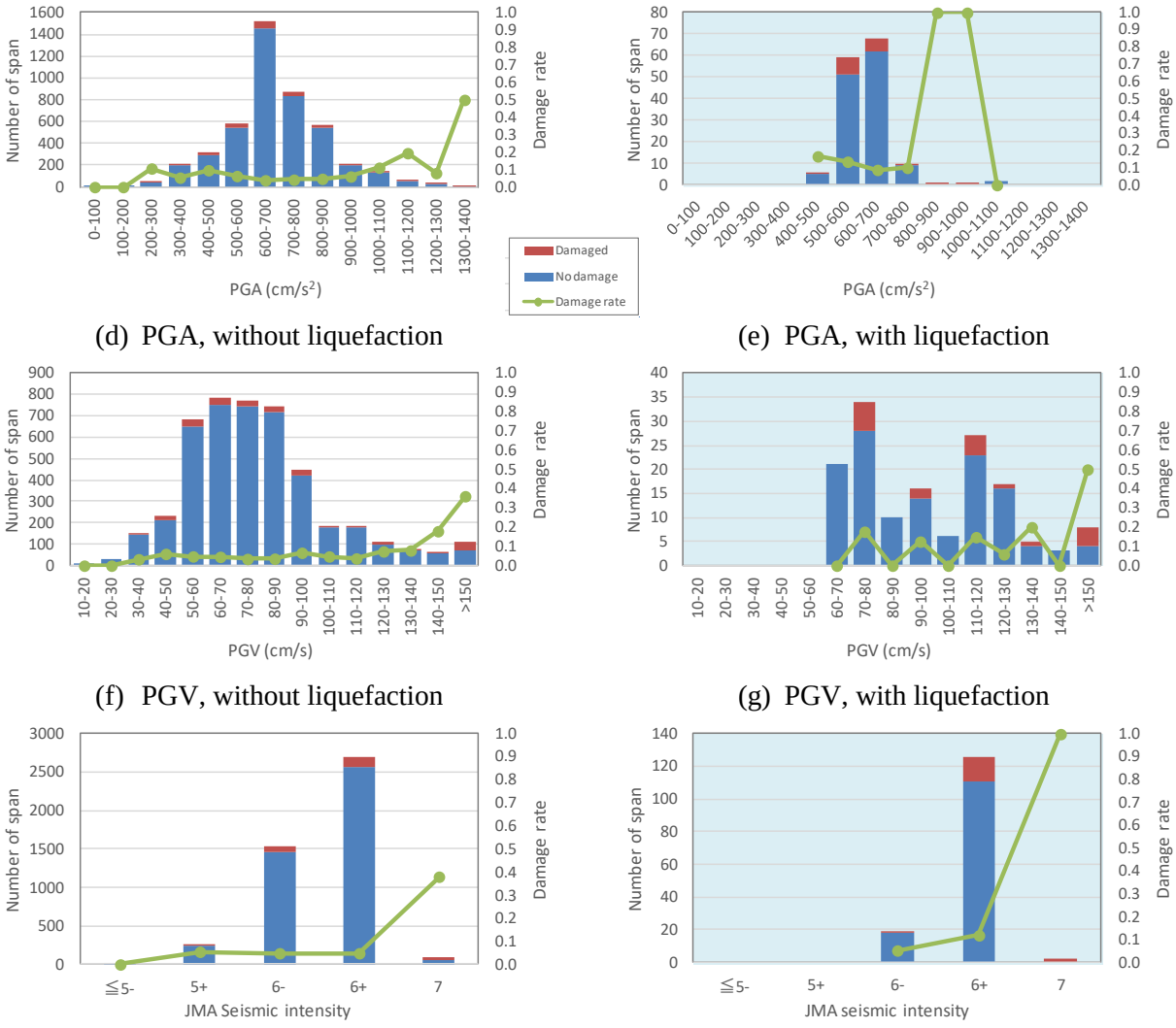

(d) PGA, without liquefaction (e) PGA, with liquefaction

(f) PGV, without liquefaction (g) PGV, with liquefaction

(h) Seismic intensity, without liquefaction (i) Seismic intensity, with liquefaction

Fig. 3 Conduit damage regarding seismic motion

3.2. Micro-terrain classification

Using the method of Shoji et al.[3], we classified the micro-topography into the 10 types listed in Table 5. Fig. 4 shows the relationship between conduit damage and topography. In terms of micro-topography, the damage rate was highest in alluvial plains, which are considered soft ground, followed by volcanic areas and volcanic foothills. Looking at the alluvial plains in detail, the damage rate was dominant in back marshes and relatively high in fans and natural embankments. One characteristic of the Kumamoto Earthquake was that the damage rate was high in volcanic foothills, which are considered better topography than back marshes. These micro-topographic categories are concentrated in Mashiki and Aso. Many surface earthquake faults have been confirmed in Mashiki, and strong earthquakes equivalent to the Great Hanshin Earthquake have been observed. On the other hand, ground deformation in Aso has been confirmed over a wide area.

Table 5 Classification of topography

Classification	J-SHIS micro-topography
Mountains	Mountain, mountain foothill, volcano, volcanic foothill
Hills	Hill, volcanic hill
Gravel terraces	Gravelly terrace
Loam terraces	Terrace covered with volcanic ash soil
Alluvial plains	Valley bottom lowland, alluvial fan, natural levee, back marsh, abandoned river channel, delta and coastal lowland, marine sand and gravel bar, sand dune, lowland between coastal dunes and/or bars, rocky shore and rock reef, dry river bed, river bed, water body
Landfill sites	Reclaimed land, filled land

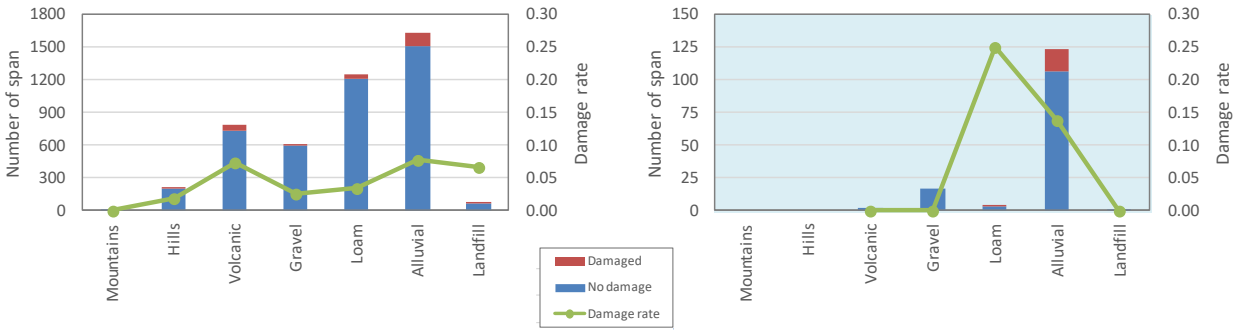

(a) Without liquefaction (b) With liquefaction

Fig. 4 Conduit damage regarding topography

3.3. Pipe types

As mentioned above, various pipe types are used in communication conduits. As listed in Table 3, we classify pipes into six types from the viewpoint of the material and joint structure: cast-iron pipe (I/PL-I), threaded-joint jute-wound steel pipe (SA), threaded-joint polyethylene-coated steel pipe (PS/S), push-on lock-joint steel pipe (PL-PS), adhesive-joint hard vinyl pipe (V), and push-on lock hard vinyl pipe (P-V). Fig. 5 shows the inspection results. The types SA, PS/S, and V, which have no expansion or contraction under the old standard, had relatively high damage rates. PL-PS also had a high damage rate. The mode of all damage was bending at joints. Although joints were bent so that the inspection equipment could not pass, no detachment was found with the pipe camera, and there was no effect on the cable.

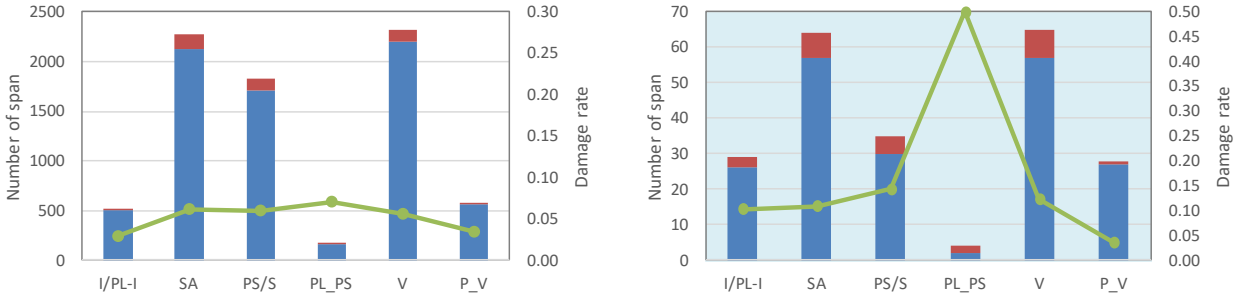

(a) Without liquefaction (b) With liquefaction

Fig. 5 Conduit damage regarding pipe type

3.4. Span length

Fig. 6 shows the inspection results by span lengths, grouped into 100-m ranges. It can be seen that the damage rate increased with the span length. This is similar to the tendency observed during the 2011 Great East Japan Earthquake. It is thought that as a span becomes longer, a greater length is affected by the seismic ground motion, making the pipe more likely to be damaged.

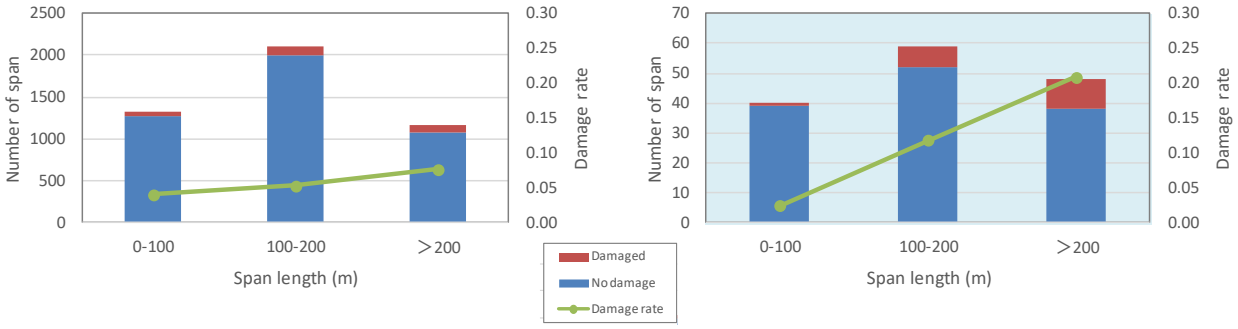

(a) Without liquefaction (b) With liquefaction

Fig. 6 Conduit damage regarding span length

3.5. Surface earthquake faults

One feature of the Kumamoto Earthquake is that many surface earthquake faults have been identified. The distance from the manholes at both ends of a conduit span to a surface earthquake fault was calculated using a geographic information system (GIS), and the shorter distance was taken as the distance from the fault to that span. Fig. 7 shows the inspection results grouped into 100-m ranges, up to 1000 m from a fault.

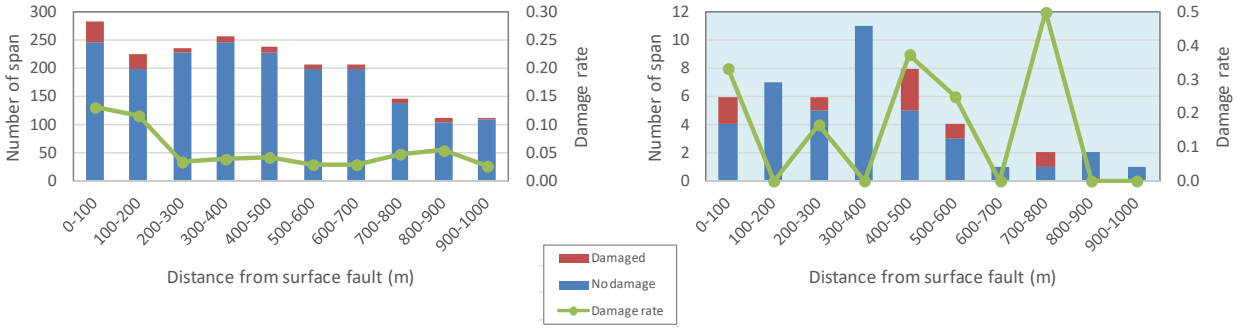

(a) Without liquefaction (b) With liquefaction

Fig. 7 Conduit damage regarding distance from surface fault

In cases without liquefaction, the damage rate was relatively high up to a distance of 200 m from a surface earthquake fault, and then it was almost flat. In cases with liquefaction, there was no clear relationship with distance, but note that the number of samples was small.

Of 103 conduit spans crossing surface earthquake faults, 32 had damage, giving a damage rate of 0.31. This damage rate is five times higher than that of the Kumamoto Earthquake overall. Fig. 8 shows the inspection results for various angles of intersection between the surface earthquake fault and the conduit span. Note that the number of samples was small. Nevertheless, the damage rate was small when the intersection angle was small, but it was high in the range of 45° to 135°, with a peak at 135°. Note that, while actual conduits may be laid in a curve to follow a road, only the coordinates of the manholes at both ends are captured in the equipment data used for the analysis. Therefore, in calculating the intersection angle, a conduit was treated as a straight line connecting two points.

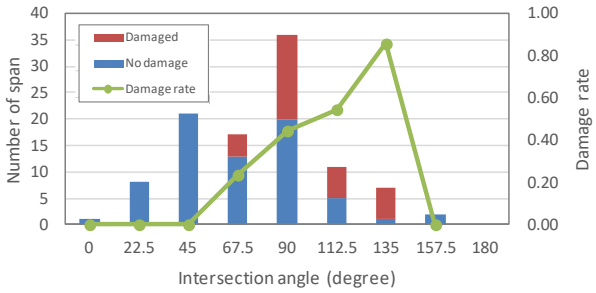

Fig. 8 Conduit damage regarding intersection angle

4. Analysis of relationships between disaster rates

By applying Shoji's research[3], the contributions of various attributes to the damage rate were calculated, and the relationships with the damage rate were analyzed. From the analysis in section 3, the damage rate differed depending on the combination of pipe type, span length, micro-topography, presence of liquefaction, and distance from a surface earthquake fault. Therefore, in analyzing the relationships, quantification of type I was applied. Qualitative data was quantified by introducing a dummy variable that became 1 only for a combination λ, and the damage rate $R_\lambda{}^*$ for each combination λ was calculated. The pipe type, span length, micro-topography classification, liquefaction occurrence status, and distance from a surface earthquake fault were items, denoted as i, with N_i denoting the number of items. The type for each item was called a category, denoted as j, with number N_{ij}. For each combination λ, a dummy variable $x_{ij\lambda}$ and a constant term c_0 were introduced. The regression model $R_\lambda{}^*$ of the actual damage rate R_λ was calculated from equation (1) below. The number of spans for a buried pipe corresponding to combination λ was denoted as L_λ, and the correction coefficient c_{ij} minimizing the objective function ε was determined by equation (2). A large value of c_{ij} meant that a parameter had a large contribution to the damage rate of the buried pipe.

$$R_\lambda^* = \sum_{i=1}^{N_i} \sum_{j=1}^{N_j} c_{ij} x_{ij\lambda} + c_0 \tag{1}$$

$$\varepsilon = \sum_{\lambda=1}^{N_\lambda} (R_\lambda - R_\lambda^*)^2 L_\lambda \tag{2}$$

Fig. 9 shows the calculation results for the correction coefficient c_{ij}. From the figure, the correction coefficient was large for steel pipe and maximal for PL-PS. For SA and PS/S with threaded joints, the damage rate was high even in past earthquakes, which is consistent with this result. Regarding PL-PS, the damage rate was low in past earthquakes, so the cause was separately examined. In the study of Shoji et al.[3], the coefficient of V was the largest, but in this study it was small. As for the span length, the coefficient tended to increase as the length increased, which is the same tendency as for the damage rate and in the research by Shoji et al.[3] The micro-topographic classification was positive for alluvial plains and volcanic terrain and had the same tendency as the damage rate. For liquefaction, the coefficient was larger with it than without it, reflecting the general tendency. The coefficient of the distance from a surface earthquake fault was negative, but it was larger within a distance of 200 m, which was also the same tendency as for the damage rate.

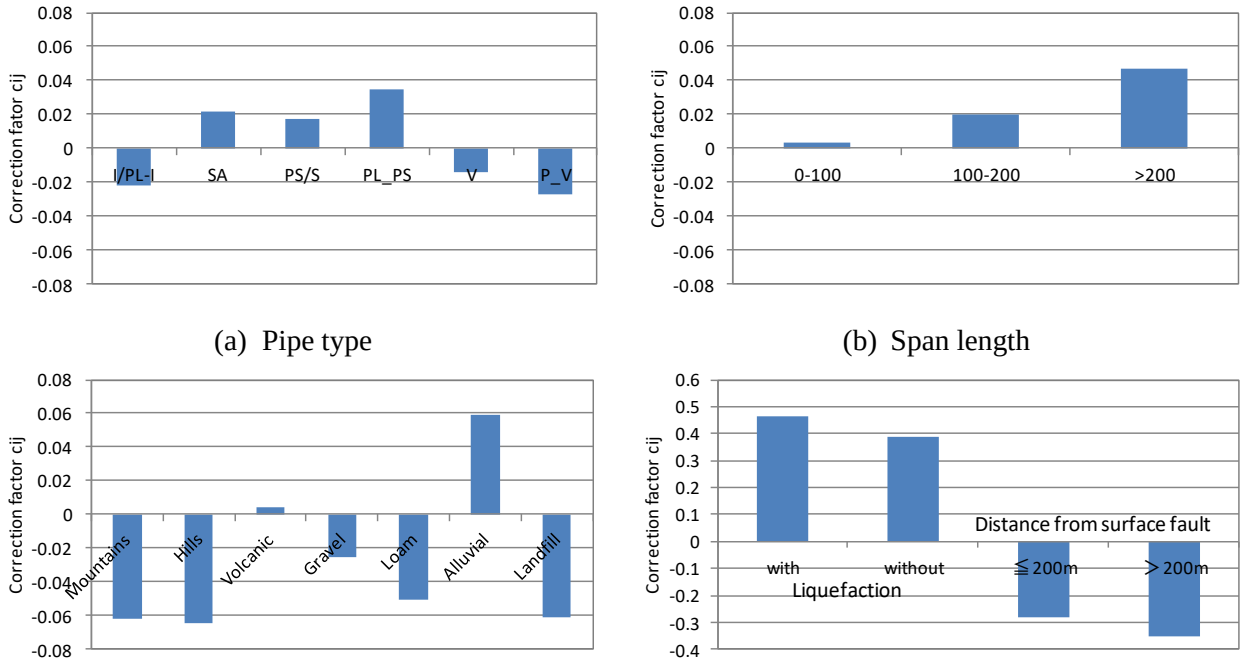

(a) Pipe type (b) Span length

(c) Topography (d) Liquefaction & distance from surface fault

Fig. 9 Correction coefficients

5. Conclusion

In this study, the damage to communication conduits during the 2016 Kumamoto Earthquake was evaluated using ground-motion intensity (PGA, PGV, seismic intensity), pipe attributes (pipe type, span length), micro-topography, liquefaction, and surface earthquake faults. The characteristics of the damage rate were analyzed from these viewpoints, leading to the following findings.

(1) The damage rate of communication conduits increases when the intensity of ground motion exceeds certain values. These values are PGA = 900 cm/s^2, PGV = 120 cm/s, and a seismic intensity of 5+. Similar trends have been seen in past earthquakes.

(2) The damage rate among the micro-terrain categories is highest in alluvial plains and also high in landfill and reclaimed lands. This tendency is also common with past earthquakes. One interesting characteristic of the Kumamoto Earthquake was the high damage rate on volcanic terrain. This is thought to relate to the large ground motion at the feet of volcanoes such as Mashiki and Aso, and to the occurrence of large-scale ground deformation.

(3) The damage rate by pipe type was the highest for PL-PS, and the next highest for standard pipes with no joint expansion/contraction capability. The current standard, PV, has a low damage rate. The tendency of

a high damage rate for old standard pipe and a low damage rate for PV is common with past earthquakes. As in past earthquakes, the damage rate tends to increase as the span length increases.

(4) The analysis also accounted for the positional relationships between surface earthquake faults and conduits, which were confirmed many times in the Kumamoto Earthquake. Without liquefaction, the damage rate is high within 200 m of a fault, after which the damage rate decreases and then levels off. The damage rate at the intersection of a conduit span and a surface earthquake fault is three times higher than the overall damage rate. Moreover, the damage rate is high in the range of pipe/fault intersection angles from 45° to 135°.

(5) By applying the theory of quantification type I, regression formulas were derived for the actual damage-rate data for each of five categories: pipe type, span length, micro-topography, liquefaction, and distance from surface earthquake faults. From the obtained correction coefficients, we consider the damage rate especially high for the following combination: steel pipe, length of 200 m, alluvial plain, liquefaction, and distance of 200 m from a fault.

6. Acknowledgements

We thank Prof. S. Katagiri of Setsunan University and Dr. Naoto Ohbo of the Association for the Development of Earthquake Prediction for their guidance and advice on this research. We also thank Dr. I. Suetomi and H. Tsukamoto of Eight Japan Technology Development for their great cooperation in our analysis. Finally, we thank the National Research Institute for Earth Science and Disaster Resilience (NIED), the National Institute of Advanced Industrial Science and Technology (AIST), and the Japan Meteorological Agency (JMA) for providing the observation data and survey results.

7. References

[1] NTT West (2018): Path to Restoration of Communication Network from the Kumamoto Earthquake, https://www.ntt-west.co.jp/universal/torikumi/torikumi08-05.html.

[2] Yamazaki Y, Segawa N, Ishida N, Suzuki T (2012): Consideration on Damage of Telecommunication Infrastructure Facilities Due to the Great East Japan Earthquake, *Japan Association for Earthquake Engineering Journal*, 12(5): 55-68.

[3] Shoji G, Kishi T, Miyazaki F, Wakatake M, Ito A, Suzuki T (2016): Clarification of Damage Mechanism for Buried Conduits of Telecommunication Systems Subjected to the 2011 off the Pacific Coast of Tohoku Earthquake, *Japan Association for Earthquake Engineering Journal*, 16(3): 213-233.

[4] Zhang Q, Wakatake M, Okutsu M, Suzuki T, Shoji G (2018): Seismic Estimation Study of Ratio of Damage to Telecommunication Conduits During Past Earthquakes, *16th European Conference on Earthquake Engineering*, Thessaloniki, Greece.

[5] Suetomi I, Tsukamoto H, Fukushima Y, Oshige J, Ohbo N (2017): Estimation of Map of AVS30 and JMA Seismic Intensity Scale During Recent Damage Earthquakes in Japan, *37th Japan Society of Civil Engineers Earthquake Engineering Symposium*, Kumamoto, Japan.

[6] National Research Institute for Earth Science and Disaster Resilience: Strong motion observation network, http://www.kyoshin.bosai.go.jp/kyoshin/

[7] Japan Meteorological Agency: Strong motion observation data, Strong earthquake observation data of major earthquakes, http://www.data.jma.go.jp/svd/eqev/data/kyoshin/jishin/index.html

[8] National Research Institute for Earth Science and Disaster Resilience (2009): Seismic Hazard Maps for Japan, http://www.j-shis.bosai.go.jp/

[9] Kataoka S, Sato S, Matsumoto S (2006): Attenuation Relationships of Ground Motion Intensity Using Short Period Level as A Variable, *Japan Society of Civil Engineers Journal*, 62(4): 740-757.

[10] National Research Institute for Earth Science and Disaster Resilience (2016): 2016 Kumamoto Earthqu ake Disaster Response Support Map, http://map03.ecom-plat.jp/map/map/?cid=11&gid=590&mid=2907

[11] Awata Y, Shirahama Y, Kumahara Y (2019): (2) Integration of surface deformation information associated with the 2016 Kumamoto Earthquake. "Comprehensive Active Fault Survey Based on the 2016 Kumamoto Earthquake, Results Report 2016-2018", MEXT Research and Development Bureau, Kyushu University.

[12] National Institute of Advanced Industrial Science and Technology (2019): Active fault database April 26, 2019. AIST Research Information Database DB095, AIST. https://gbank.gsj.jp/activefault/

